Experimental Investigation of Flame Kernel in Turbulent Partial Premixed Flames

A. M. Elbaz   ayman_alhagrasy@m-eng.helwan.edu.eg
Faculty of Engineering/Mechanical Power Engineering Department
Helwan University
Cairo, 11718, Egypt

Mohy Mansour   mansour@niles.edu.eg
Faculty of Engineering/Mechanical Power Engineering Department,
Cairo University, Egypt

Diaaeldin Mohamed   diaa.eldin@aucegypt.edu
Faculty of Engineering/Mechanical Power Engineering Department,
Cairo, University, Egypt

Abstract

The flame kernel propagation is believed to be influenced by many operating parameters such as mixing level, turbulent intensity, and the mixture equivalence ratio. The purpose of this study is to investigate the effect of the mixture equivalence ratio and turbulence intensity on the flame kernel and flow field interlinks in partially premixed natural gas flames. Three jet equivalence ratios of 1, 1.5, and 2 are considered at values of jet velocities in the range from 10 to 20 m/s. This study was done under constant degree of partial premixing. A pulsed Nd: YAG laser is used for the flame ignition, and the turbulent flow field is captured at several time intervals from ignition using two-dimensional Planar Imaging Velocimetry (PIV). The mean flow field doesn't influence with the flame kernel propagation. The turbulent flow field indicates an increase in the global turbulence intensity in flames associated with the kernel propagation in comparison with the isothermal case. The jet equivalence ratio of one enhances the flame kernel propagation and it gives the highest rate of kernel propagation. Increasing the jet equivalence ratio to 1.5 and 2 reduces the intensity of chemical reaction and hence the effect of turbulence becomes the dominant factor effecting the propagation of the flame kernel .At jet velocity of 20 m/s , an early flame kernel extinction is recorded without any respect to jet equivalence ratio. At the early stage of the kernel generation at delay time of 150 µs, linear correlation between the jet velocity and the kernel propagation is noticed. The chemical reaction is the main factor influences the rate of kernel propagation; it gives nearly 3.5 times the effect of the flow convection to the maximum rate of the flame kernel propagation at jet velocity of 20 m/s and equivalence ratio of one.

Keywords: Flame kernel, Partial premixed flame, PIV, Flow field.

1. INTRODUCTION

The early phase of combustion in spark ignited combustion systems affects the flame propagation and stability, and hence the performance, of the combustion process and the system efficiency. The developing flame kernel represents this phase and is affected by many parameters, such as spark energy, rate of energy release, turbulent flow field and the fuel/air mixing. Previous studies have shown that variations in the initial growth of the flame kernel contribute significantly to cycle-to-cycle variation in engine performance and emissions [1]. The flame kernel has attracted many experimental research groups [2, 3-5] and DNS research groups [4, 6-9] interested in studying flame kernel evolution in turbulent environmental and the main factors that control its characteristics and propagation. Many parameters have been investigated to study their effects on the flame kernel characteristics and propagation, e.g., flame shape, wrinkling and curvature. In the following section a brief review of these studies and their findings are presented and discussed.

Katta et al. [10] reported an experimental and numerical investigation using a unique counter flow diffusion flame with an embedded vortex generator. This study was to understand the local quenching process associated with the vortex-flame interaction in methane diffusion flames. The results show that, the high increase in CH3 radicals in the strained flame zone depleted the radical pool (such as OH, H, and O) and, hence, the flame is quenched locally. They concluded that this quenching process is different from the quenching observed in steady counter flow flames, where the quenching was due to the gradual reduction in temperature with increasing strain rate. Renard et al. [11] investigated experimentally (using OH PLIF) the flame front of a non-pre-mixed flame interacting with a vortex to study the heat release, extinction and time evolution of the flame surface. They concluded that global intensification or extinction of the flame is characterized by an increase or decrease in flame surface area because of straining. Marley et al. [12] investigated experimentally the interaction of spark-ignited flame kernels with a laminar vortex. They concluded that burning rates for rich flames were decreased, with total flame kernel extinction occurring in extreme cases. They also proved that small flame kernel–vortex interactions are dominated by transient stretch effects and thermo-diffusive stability, in agreement with premixed flame theory. Furthermore, they pointed out that vortex interactions with larger methane–air flame kernels led to slight flame speed enhancements for both lean and rich flame kernels.

Furthermore, Arcoumanis et al. [13] showed that using a small quantity of rich mixture injected near the spark gap can yield to formation of a stable and consistent flame kernel after spark ignition. The function of this local variation in equivalence ratio is to support the flame in a mixture with an overall equivalence ration as low as 0.39. They concluded that not only the average flame speed could be increased by local injection at all equivalence ratios [14] but also the fluid dynamic effect alone caused overstretching of the flame for the ultra lean homogeneous conditions, while rich local stratification in the vicinity of the spark allowed the suppression of this effect and a reduction of the drivability limit [15]. Roberts et al. [16-18] investigated the added complexity of flame kernel–vortex interactions compared to some earlier planar flame–vortex configuration. They observed experimentally the initial flame kernel–vortex interactions using OH-PLIF in a lean atmospheric-pressure methane–air flame kernel to determine the degree of flame wrinkling and the ability of vortices of varying size and strength to globally quench combustion [16].The disturbed flame existed in either the flamelet regime (which has a continuous reaction zone) or distributed reaction zone regime (which has a coexistence of reactants and products) is strongly dependent upon: the vortex size, the vortex strength, and the time of the initial flame–vortex interaction. They investigated the global extinction of the flame kernel with large vortex sizes interacting with small flame kernels. In addition to that, they concluded that the localized flame front extinction occurred for a range of vortex sizes and strengths and a range of flame kernel sizes.

Meanwhile, Thevenin et al. [19] and Renard et al. [20] reported an experimental and numerical work of non-premixed flame interacting with a vortex. They investigated the influences of global mixture ratio and vortex velocity on changes in the flame surface. Their study concluded that straining effects are responsible for the extinction of the non-premixed flame front, and the degree of mixing actually increases at the end of the extinction process. They were able to observe the fuel pocket formation, evolution and consumption are another important phenomenon during flame-vortex interactions. In addition to that, the causes for local flame quenching were reported by (Patnaikand Kailasanath [21]) as well. They concluded that these causes happen due to simultaneously high strain and the heat losses in flame-vortex interactions of lean methane/air mixture. Harinath Reddy and John Abraham [22] studied the outcomes of interactions of counter-rotating vortex pairs with developing ignition kernels. They examined quantitatively and qualitatively the evolution of flame surface area during kernel–vortex interaction. They pointed out that flame development is accelerated and the net flame surface area growth rate increased with increasing vortex velocity, besides they proved that increasing the vortex length scale increases the surface growth rate. They noticed when the vortex velocity is high relative to the flame speed, the vortex breaks through the ignition kernel carrying with it hot products of combustion, which accelerates growth of the flame surface area and heat release rates compared to a kernel with no vortex interaction.

Recently, experimental work on the flame kernel structure and propagation in a high turbulent premixed methane flow was performed by Mansour et al. [23] using combined two-dimensional Rayleigh and LIPF-OH techniques. They generated the spark of ignition using pulsed Nd: YAG laser. They investigated four flames at two equivalence ratio of 0.8, and 1, and jet velocity of 6, and 12 m/s.

A. M. Elbaz, Mohy Mansour & Diaaeldin Mohamed

They showed that the flame kernel structure starts with spherical shape, and then changes gradually to peanut-like, then changes to mushroom-like and finally the turbulence effectively distributes the kernel. They concluded that the trends of the flame propagation, flame radius, flame cross section area, and mean flame temperature are correlated to the jet velocity and equivalence ratio, also lean flames propagate faster.

Based on this review of previous researchs, it is notable that the interaction between the flow field and flame kernel propagation hasn't been investigated experimentally in high turbulent partially premixed flames. Thus, the aim of the present work is to investigate the flow field associated with flame kernel propagation history in partial premixing turbulent flames. The experimental program is devoted to study the effect of the jet equivalence ratio and turbulence intensity on the flame kernel and flow field interlinks in partially premixed natural gas flames. The mean flow field and turbulence intensity are measured using two-dimensional Planar Imaging Velocimetry (PIV), in terms of mean axial velocity and rms. The flow field is first captured for the isothermal field without ignition accompanied, and this could be used as a reference flow field to those flow fields with ignition. The flow field with ignition is recorded after the start of ignition at different delay times. Therefore, the flame kernel-turbulent flow field interaction could be interpreted by the comparison of flow fields of the isothermal and ignited cases.

2. EXPERIMENTAL TECHNIQUE

As shown in Fig.1a, the burner consists of two vertical concentric stainless steel tubes of 6 mm and 10 mm inner diameters and tip thickness of 1 mm. Air is passing through the inner tube while the fuel (natural gas of 95% CH4 by volume) flows through the annular passage between the inner and outer tubes. The inner tube exit is lower than the exit of the outer tube by a distance L. This distance can be varied to generate different degree of partial premixing. Mixing starts at the exit of the inner tube and continues downstream along the premixing distance L. The burner is sitting at the top of conical turbulence generator as shown in Fig. 1a which is similar to Videto and Santavicca [24] turbulent generator, the flow passes through a narrow slit at a diameter of 45 mm and a slit thickness b = 0.8 mm, followed by an inverted cone with 52° base cone angle. The coming flow from the slit provides a ring-like cylindrical shape, which is broken at the inner cone wall to generate a wide range of eddies, which leads to higher turbulence intensity. The turbulence intensity due to this burner concept can be as high as 25% [24]; this is confirmed by the turbulent flow field measurement at the burner exit. The current Planar Imaging Velocimetry technique, explained in details below, requires to image seeding particles within the flow. However, due to the narrow slit dimension of the turbulence generator, it isn't possible to pass all the seeded flow through the slit. Therefore, 10 % of the total air flow rate is used to carry the seeding particles and passes through a central concentric tube with the turbulent generator disk, as shown in Fig. 1a, while the rest of the air flow rate is passed through the slit. Then both streams are mixed inside the cone. Titanium dioxide with a mean diameter of 0.5 μm is used as seeding particles through a fluidized bed seeder.

The interactions between the flame kernel and flow field is investigated at several delay time intervals from ignition, under different jet equivalence ratio and jet velocity. This is based on capturing the turbulent flow field after the ignition at different delay time, namely 150, 300, 500, 1000, 1500, and 2500 μs. These flow fields are compared with flow field without ignition (henceforth to be termed isothermal flow) to identify the effects of the evolving flame kernel. A pulsed Nd:YAG laser (Continuum Surelite II) is used for flame ignition, see Fig.(1-b). Laser ignition provides more stable measurable pulse energy, and overcome the problems of the effects of spark electrodes on the flame structure, as well as heat loss to the electrodes. The laser provides a beam of 6 mm diameter at 1064 nm with 230 mJ and is focused to a beam of waist radius of 5.6 μm using spherical lens of 50 mm focal length.

As shown in Fig.(1-b), the flow field is measured using two-dimensional Particle Imaging Velocimetry (PIV) technique, of two head Nd:YAG laser with pulse energy of 50 mJ at the second harmonic of 532 nm. The camera is HiSense Mkll PIV CCD cameras (model C8484-5205CP) with 1280 x 1024 CCD light sensitive array and equal number of storage cells. The objective of the camera is covered with interference filters at 532 nm with a bandwidth of 10 nm. The laser pulse duration is 6 ns and the inter-pulse delay between the two laser heads is controlled according to the flow velocity with a minimum of 0.2

µs for supersonic flow. The laser sheet is created by sheet forming optics that produces expanding laser sheet. Timing between the laser ignition, the PIV laser sheet forming and the camera capturing was controlled by 4 channel Stanford Research DG535 pulse delay generator and monitored with a Tektronix 4 channel 200 MHz oscilloscope. The PIV images were processed using an adaptive window offset cross-correlation algorithm implemented in a commercial analysis package (Dantec Dynamic Studio V 2.30). The final interrogation window was 32×32 pixels with a 50% window overlap, resulting in a spatial resolution 1.5 mm and vector spacing of 0.5 mm.

FIGURE 1: a) The burner, b) The experimental set up.

3. FLAME STABILITY AND SELECTED CONDITIONS

Flame extinction can be approached by either increasing the jet velocity for the same fueling rate or reducing the equivalence ratio at the same jet air velocity. In the present work the degree of partial premixing is fixed where the premixing length L is kept constant at L/D = 2 for all cases, where D is the inner diameter of the outer burner tube. Figure 2 illustrates the stability characteristics of the burner, where the stability point is achieved via gradual decrease of the fuel flow until the flame blows off, while preserving the air flow rate constant. The results are presented as a relation between the jet velocity (Uj) and the jet equivalence ratio (Φj). The results depicted in Fig. 2 shows that the higher the jet velocity, the higher the corresponding jet equivalence ratio required for stable flames.

In relevance with the stability limit, the flame kernel and the turbulent flow fields are investigated at three jet equivalence ratio of 1, 1.5 and 2. For each equivalence ratio, five different jet velocities are applied and investigated beginning from 10 m/s to 20 m/s with increasing step of 2.5 m/s, see Fig. 2. The flow

conditions are listed in Table 1. The flames are selected on the unstable region, and the flame kernels are ignited and propagated after each laser pulse. Since this is unstable flame region, this allows the recording ability of the flow fields at several times from the ignition during the flame kernel propagation, without the need to shut down the flame. The flow fields of the previous flames are also examined without ignition (isothermal flow conditions) to be used as references of comparison with those flow fields accompanied by flame kernel.

Uj(m/s)	$\Phi j=1$	$\Phi j=1.5$	$\Phi j=2$
10	√	√	√
12.5	√	√	√
15	√	√	√
17.5	√	√	√
20	√	√	√

Table 1: The selected flames conditions

*The flame designation is FΦj-Uj, where, the symbol Φj after F indicates the jet equivalence ratio, while the second number represents the jet velocity. For example, F1-10, it means the jet equivalence ratio equals 1 and jet velocity equals 10 m/s. The isothermal case is indicated by adding a superscript iso to the previous acronym, like F2-10^{iso}, it means at those flow conditions the turbulent flow field is recorded without ignition.
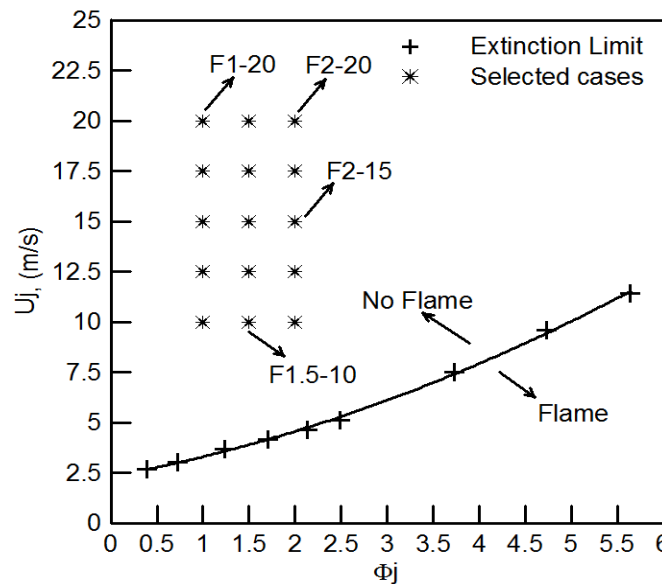

FIGURE 2: Stability limit and the selected flame conditions

4. RESULTS AND DISCUSSION

The contours of the normalized mean axial velocity U/Uj of isothermal jet flow and the ignited cases of flame F2-10 are illustrated in Fig. 3a at several time intervals from ignition,[the isothermal case is located at the left of the figure while those on the right are the time history of the mean velocity fields of the ignited cases]. As shown for the mean flow field, there is no any difference between the isothermal case and the ignited cases at any delay time from the ignition. For the isothermal and the ignited cases, the flow field is featured by a central core region extending to a nearly axial distance of 2D (D is the inner diameter of the outer nozzle), with axial velocity of nearly U/Uj=1.2. The core flow region is surrounded by annular mixing region, which merges downstream the end of the potential core region. This result demonstrates that the flame kernel propagation has no effect on the mean flow field.
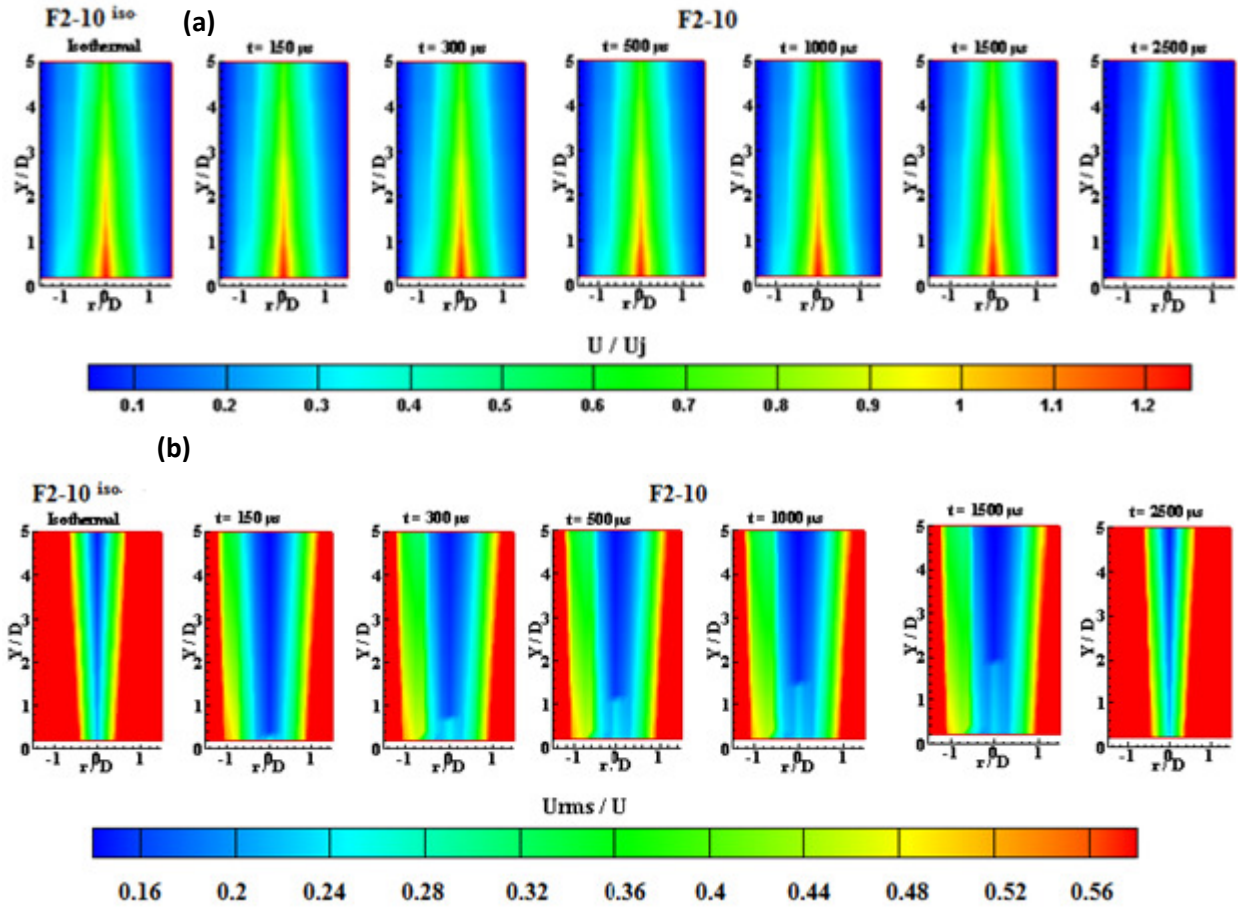
FIGURE 3: (a) Contours of the normalized mean axial velocity (U/Uj) for isothermal, at the left hand side and the ignition cases at several time intervals from ignition in flame F2-10, at the right of the isothermal case, (b) Contours of the normalized rms (Urms/U) for isothermal, at the left hand side and the ignition cases at several time intervals from ignition in flame F2-10.

On the other hand, as shown in Fig. 3b the contours of the turbulent intensity in terms of Urms/U, shows a significant difference between the isothermal and the ignited cases. This can be seen by the higher turbulence intensity along with the jet centerline in case of the ignited cases at any delay time from the ignition with respect to the isothermal case. This central region of the higher turbulence intensity is propagated in the range of the delay of 150 to 1500 µs, and shows a maximum propagation axial distance at 1500 µs. After this time the turbulent flow field returns again to the original turbulence state at time delay of 2500 µs, as the isothermal case (see the first and the last contours of Fig. 3b). This result indicates that the flame kernel affects the turbulent flow field. Other feature of the turbulence intensity field associated with the flame kernel propagation is the increase of the width of the radial distribution of the turbulence intensity in the range of Urms/U (from 0.16 to 0.56), this turbulence intensity range is spanning a narrow radial distance in the isothermal case with the comparison of the ignited cases at any axial distances. This means that the flame kernel propagation leads to the redistribution the turbulent kinetic energy.

Figure 4 illustrates the radial profiles of the turbulence intensity of flame F2-10 at delay time of 1000 µs at three axial distances, namely at the point of the sudden decay of turbulence intensity which can be taken as a trace of flame kernel propagation, X, while the other two locations upstream and downstream X, by 2 mm, X-2, X+2, respectively. The close inspection of the profiles shows that the turbulence intensity is

relatively high along the flame centerline at X-2 and X. More outward displacement from the jet centerline, the turbulence intensity showed a slight decrease reaching a minimum turbulence intensity point, and this indicates that the kernel centerline is associated with higher turbulence intensity. Beyond the radial location of the point of minimum turbulence intensity, the turbulence intensity starts to increase and merges with the profiles of the turbulence intensity of the axial position at X+2. Where the turbulence intensity profile at X+2 shows a minimum value at the jet centerline, which is similar to the ordinary jet flow. This indicates at the axial position of X+2, the kernel is extinguished, which indicates the reasons behind the radial stretching of the turbulence intensity profiles in the case of the ignited flame kernel with the comparison to the isothermal one.
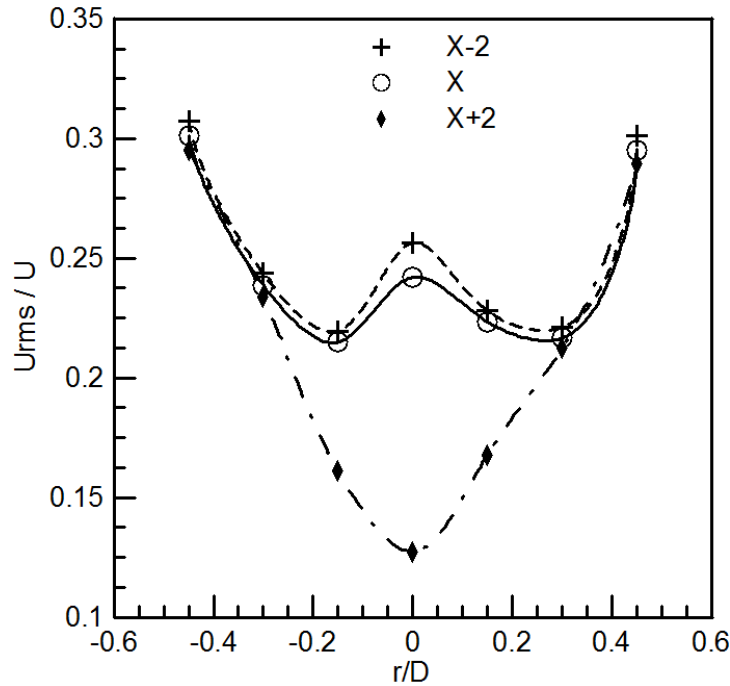

FIGURE 4: Radial distribution of axial turbulence intensity at different axial locations: upstream the flame kernels limit X-2, at the flame kernel limit X, and at downstream the kernel X+2 of flame F2-10 at delay time = 1000 μs.

Fig. 5 shows the centerline turbulence intensity for the jet equivalence ratio of one and jet velocity of 10 m/s at different time of delay from the ignition, with the comparison with the isothermal case. As seen as the flame kernel propagates as it delays the steep decay point of the turbulence intensity, and by this way the flame kernel could be traced. At jet velocity of 10 m/s, increasing the jet equivalence ratio from 1 to 1.5 and 2 shows similar qualitative turbulence intensity change, as compared to the corresponding isothermal cases, see Fig. 6. To quantify the effect of the jet equivalence ratio on the turbulence intensity accompanied with the flame kernel propagation. This turbulence intensity along the jet centerline for the three equivalence ratios at delay time of 1000 μs and jet velocity of 10 m/s is illustrated in Fig.7. All of these centerline turbulence intensities are compared to the isothermal case in the same figure. In general, centerline turbulence intensity of the isothermal case shows nearly linear decrease in turbulence intensity along the axial distance. While, for the three equivalence ratios of the ignited cases, the centerline turbulence intensity is noticed to be higher at the early axial distance, which also shows a mild decrease in the turbulence intensity along with the increase in the axial distance. This mild decline in the turbulence intensity is changed into a steep decrease in the turbulence intensity to a lower level of turbulence intensity; but this level is still higher than those recorded in the isothermal case.

As mentioned before, the axial location of the steep decrease in the centerline turbulence intensity can be taken as an indication of the flame kernel propagation. The high turbulence regime may be occurred due to flame kernel fluctuation in this region and this should be associated with large rms and consequently high turbulence intensity. In addition, the interaction between the flame kernel and flow field likely causes disturbance and hence another factor affects the turbulence intensity. Thus, the position of the decrease

of the turbulence intensity can be used as the mean position of the flame kernel, (this will be demonstrated later in the section of the rate of flame kernel propagation).
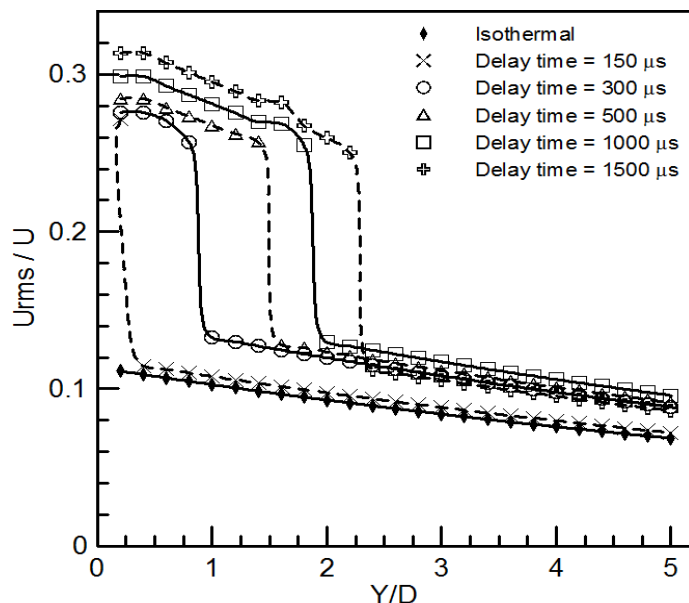

FIGURE 5: The centerline Urms/U for F1-10 at different time of delay and the corresponding isothermal case

As shown in Fig. 7, the jet equivalence ratio of 1 gives the highest flame kernel propagation while it decreases by increasing the equivalence ratio. This is consistent with variation of the flame speed with the gradient in the equivalence ratio. This reflects the effect of fuel-air chemistry on the flame kernel propagation, where the partial premixed mixture with jet equivalence ratio of 1 sustains the flame kernel propagation. This could be explained on the basis of the higher chemical reaction rate of the stoichiometric mixture to withstand the turbulence effect. On the other hand, increasing the jet equivalence ratio decreases the chemical reaction rate and hence the effect of turbulent on the flame kernel becomes predominate, this affects the kernel propagation and its rate.

With the respect to the flame kernel propagation and the rate of propagation, Fig. 8 shows a comparison between our results and those results of Mansour et al [23]. The results of Mansour et al. [23] are based on using a combined two-dimensional Rayleigh and LIPF-OH technique. Where, the average axial locations of the flame kernel center, obtained from all 200 images of LIF-OH measured in each flame. The results show an excellent agreement between our data and the compared ones up to delay time of 300 µs, while after this delay time the two trends are qualitative similar with a slight increase in our kernel propagation, and this is believed due to the slight increase in our selected jet velocity by 0.5 m/s, which enhances the kernel propagation, as well as, the results of Mansour et al [23], were performed on a premixed mixture.

The effect of both jet velocity and jet equivalence ratio on the flame kernel propagation and the rate of the flame kernel propagation can be understood from Figs. 9 and 10, respectively. In Fig. 9, the flame kernel propagation distance Z in mm is represented on the vertical axis versus the jet velocity on the horizontal axis at each delay time from the ignition. The results indicate that the flame kernel propagation increases with increasing the jet velocity at any delay time from ignition, and this is attributed to the higher convection effect of the flow with increasing the jet velocity.

At early stage of the flame kernel generation at time lag of 150 µs a linear correlation between the jet velocity and flame kernel propagation is recorded for the three jet equivalence ratio. Beyond this time lag of 150 µs, a deviation from the linear correlation between the jet velocity and the kernel propagation is noticed and the nonlinearity increases with increasing the delay time. This may be explained based on the results of Mansour et al [23], where the shape of the flame kernel at the early delay time is not affected by turbulence and hence this reduces the effect of turbulence level on the flame kernel propagation at the early time of flame kernel generation. At this early time stage the flame kernel is

almost spherical. After some more time the flame kernel shape is corrugated and takes different shape, and hence the effect of the turbulence intensity of the flow field is predominate and the flame kernel boundaries is affected more by the turbulence eddies.
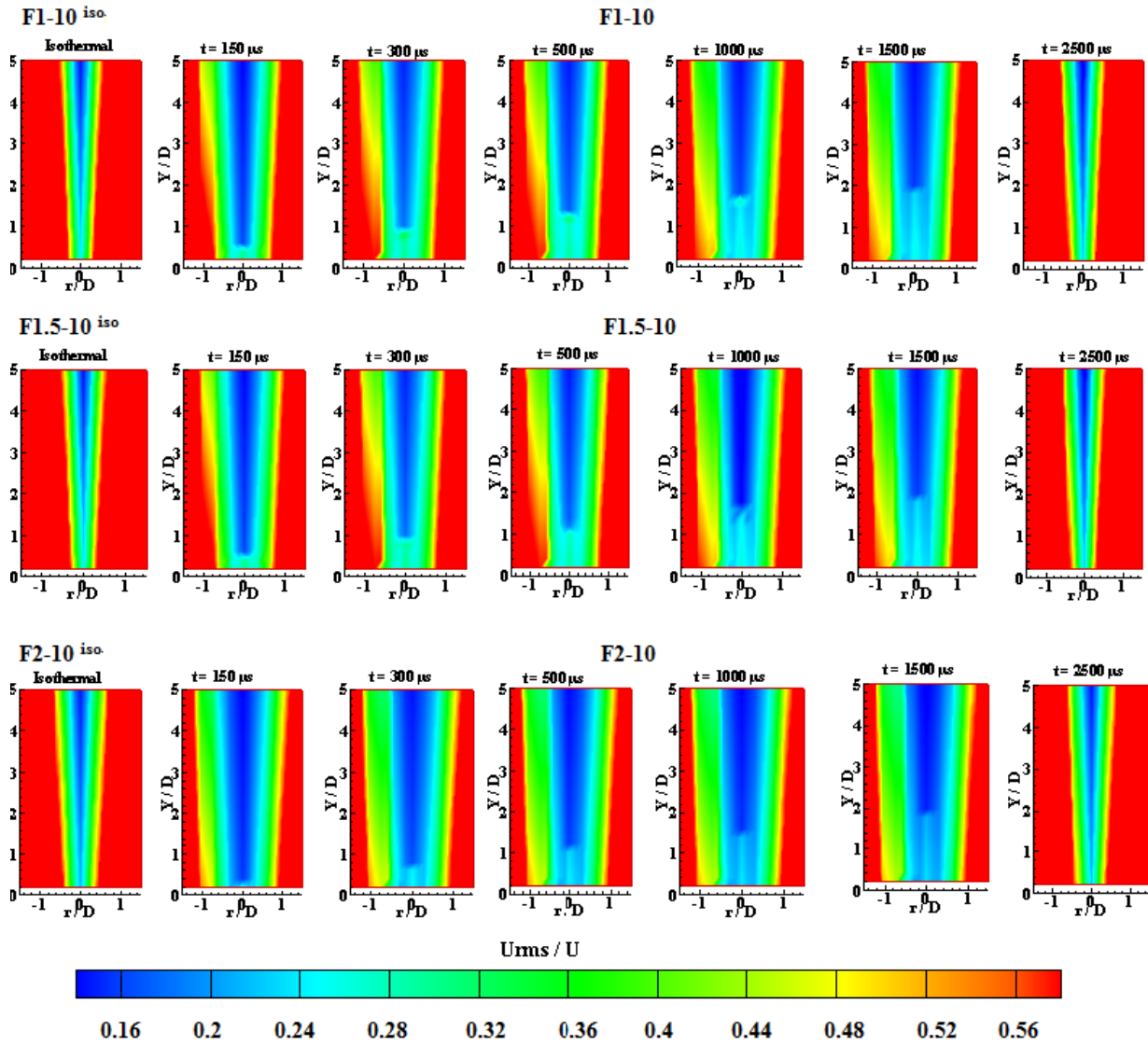

FIGURE 6: Contours of the axial turbulence intensity Urms/U of flame F1-10, flame F1.5-10 and flame F2-10 (from top to bottom, respectively)
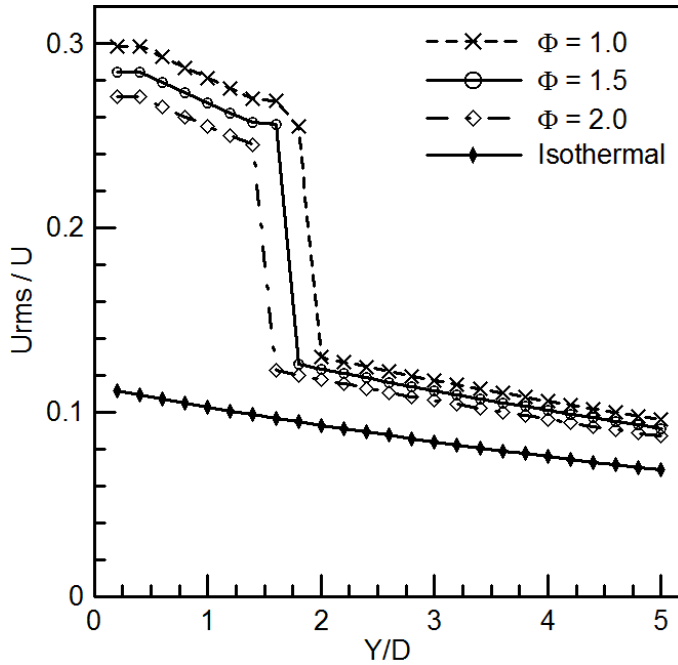
FIGURE 7: Centerline axial turbulence intensity at Uj = 10 m/s with Φ_j = 1, 1.5, and 2, at delay time of 1000 μs with comparison to the isothermal case.
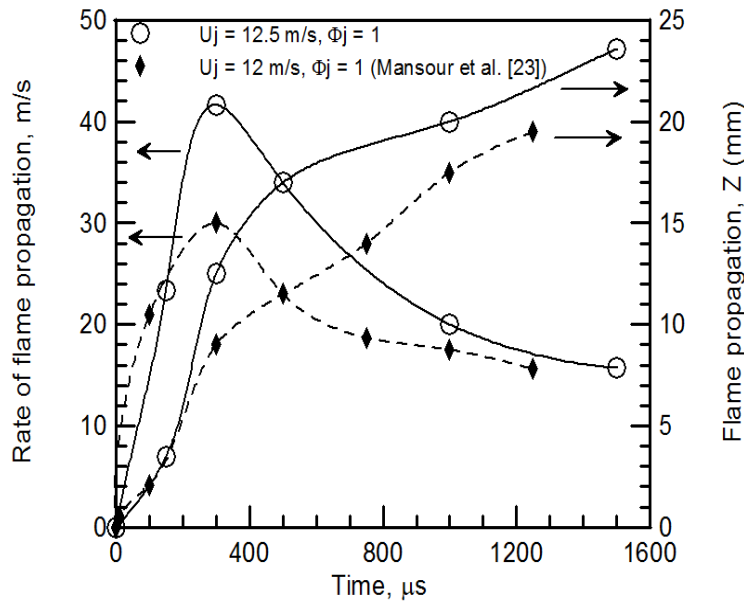

FIGURE 8: The flame kernel propagation and rate of flame kernel propagation at Φ_j =1, and Uj=12.5 m/s, compared to Mansour et al [23], at Φ_j =1, and Uj=12 m/s.

The above results can be reflected on the flame kernel propagation rate, see Fig. 10, the data provides an illustration of the flame kernel propagation rate in m/s (vertical axis) at different delay times presented on the horizontal axis. The results show that the rate of flame propagation increases with respect to the time in steep manner till reaching a maximum rate at nearly 300 μs for all jet velocity. This maximum rate increases with increasing the jet velocity due to the higher convection effect. After this point of maximum

rate, the flame kernel propagation rate is attenuated with increasing the time lag. This decay in the rate of flame propagation is very clear at the higher jet velocity see jet velocities of 17.5 and 20 m/s in Fig. 10. This indicates that increasing up to these high jet velocities of 17.5 and 20 m/s, increases the turbulence intensity to a level which leads to the weakness of the chemical reaction, where the chemical reaction can't withstand these high rates of reactants. At the same time the higher the jet velocity leads to more local turbulence intensity in the location of the kernel, which in turn increases the heat dissipated to the surrounding and the kernel extinction occurs. This could be highlighted by the relative early flame kernel extinction at the jet velocity of 20 m/s without any relevance to the mixture equivalence ratio. If the maximum rate of flame kernel propagation is normalized by the exit jet velocity, it will indicate the effect of the chemical reaction for the flame kernel rate of propagation. At the jet velocity of 20 m/s and jet equivalence ratio of 1, the ratio of the maximum rate of flame kernel propagation to the exit jet velocity is nearly 3.5; this proves that the chemical reaction enhances the rate of flame kernel propagation more than the coming from the convective effect of the flow field.
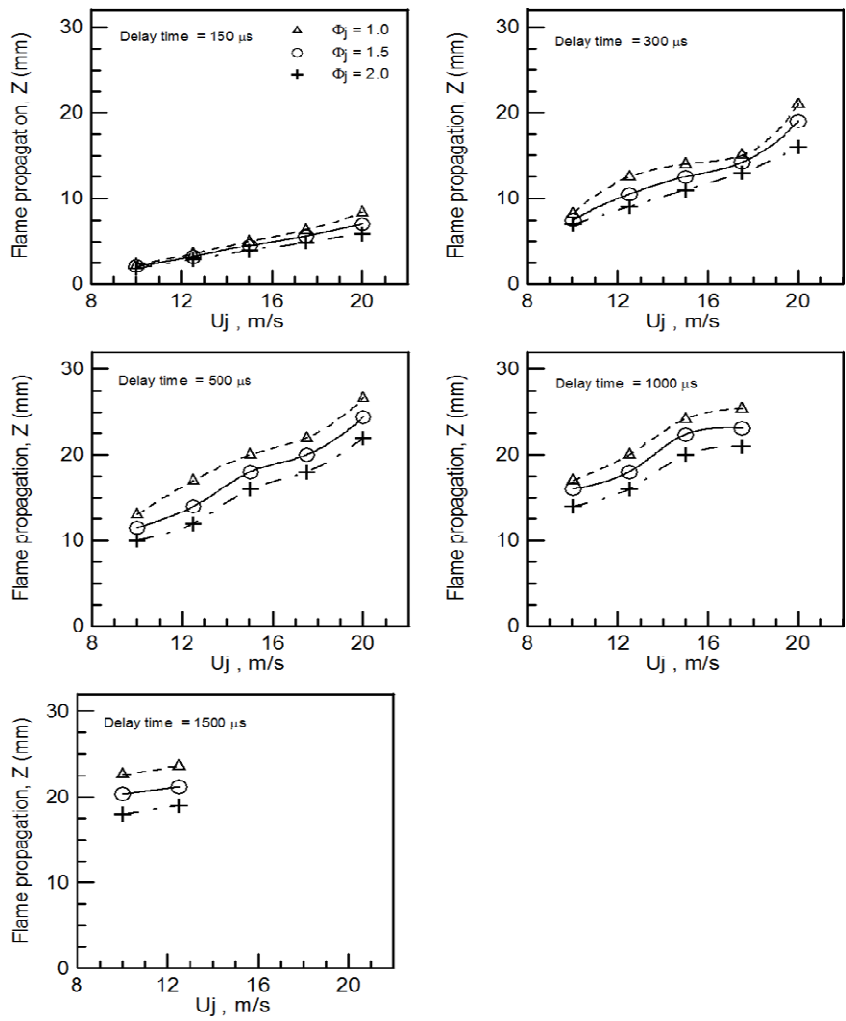

FIGURE 9: Flame kernel propagation at ΦJ =1, 1.5 and 2 for different delay times.
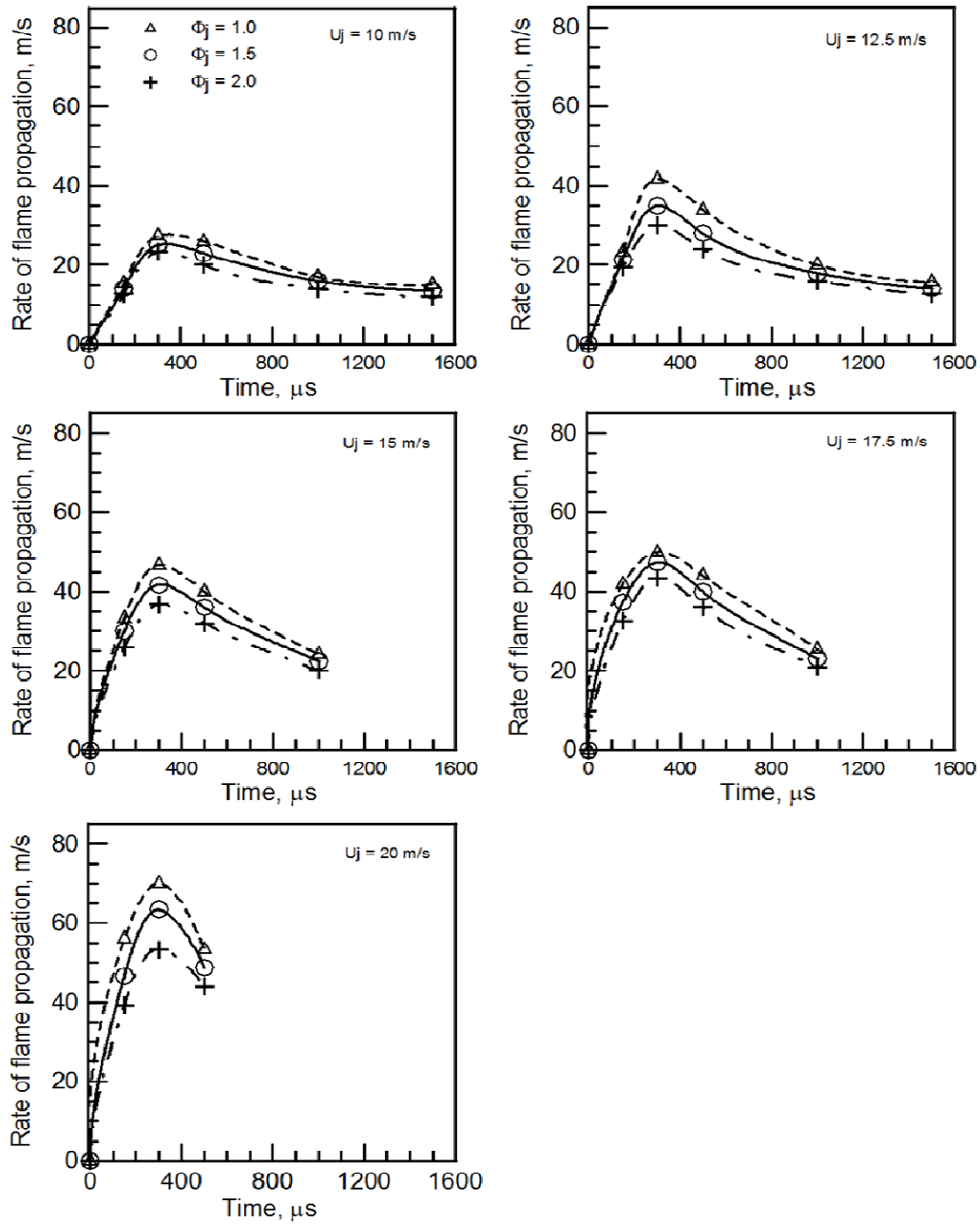
FIGURE 10: Rate of Flame kernel propagation at Φj =1, 1.5 and 2 for different jet velocities.

5. CONCLUSIONS

An experimental work is conducted on the flame kernel propagation of partial premixed natural gas turbulent flames under a constant degree of partial premixing. The study is oriented to study the effect of jet equivalence ratio and jet velocity on the flow field-flame kernel interaction. The mean flow field and turbulence intensity are measured using two-dimensional Planar Imaging Velocimetry (PIV). The flow field is captured for the isothermal field without ignition in order to be used as a reference to those flow fields with flame kernel. The flow field with ignition is recorded after the start of ignition at different delay times. The data show that the mean flow field isn't affected by the flame kernel if it is compared to the isothermal one. It is found that the centerline turbulence intensity increases during the flame kernel propagation, and then followed by a sudden decrease. The flame kernel propagation and its rate in the stoichiometric flames are occurred at higher rates compared to the richer flames. This is consistent with the flame speed

data where the maximum flame speed occurs at the stoichiometric cases. This leads to more significant effect of turbulence on the flame kernel propagation at richer conditions. During the early period of the flame kernel generation, within the first 150 µs period, a linear correlation between the jet velocity and flame kernel propagation is recorded for all equivalence ratios. Beyond this period of 150 µs, a deviation from the linear correlation between the jet velocity and the kernel propagation is noticed and the nonlinearity increases with increasing the delay time. This indicates that flame kernel propagation is accelerated. Moreover, increasing the jet velocity up to nearly 17.5 m/s and more,   increases the turbulence intensity to a limit which weakens the chemical reaction, which can't withstand this higher rates of reactants. The relative early flame kernel extinction at the jet velocity of 20 m/s is occurred without any relevance to the value of jet equivalence ratio.

6.   ACKNOWLEDGEMENTS

7. FUTURE WORK

To go more depth about the flame kernel and flow field interaction, planar laser-induced fluorescence (PLIF) and stereoscopic particle image velocimetry (PIV) will applied at 10 KHz repletion-rate to acquire time-resolved of the flow field flame kernel interaction.

8.   REFERENCES

[1] R.R. Maly, in: J.C. Hilliard, G.S. Springer (Eds.), "Flow and Combustion in Reciprocating Engines," *Plenum Press, New York,* 1983.

[2] C.F. Kaminski, J. Hult, M. Alden, S. Lindenmaier, A. Dreizler, U. Mass, M. Baum, "Complex turbulence/chemistry interactions revealed by time resolved fluorescence and direct numerical simulations," *Proceedings of the Combustion Institute* 28:399–405(2000).

[3] A. Dreizler, S. Lindenmaier, U. Maas, J. Hult, M. Alden, C.F. Kaminski, "Characterization of a spark ignition system by planar laser induced fluorescence of high repetition rates and comparison with chemical kinetic calculations," *Applied Physics* B70:287–294 (2000).

[4] S. Gashi, J. Hult, K.W. Jenkins, N. Chakraborty, R.S. Cant, C.F.Kaminski, "Curvature and wrinkling of premixed flame kernels – comparisons of OH PLIF and DNS data," *Proceedings of Combustion Institute* 30:809–817 (2005).

[5] C.C. Huang, S.S. Shy, C.C. Liu, A. Yan, "A transition on minimum ignition energy for lean turbulent methane combustion in flamelet and distributed regimes," *Proceedings of the Combustion Institute* 31:1401–1409(2007).

[6] K.W. Jenkins, R.S. Cant, "Curvature effects on flame kernels in a turbulent environment," *Proceedings of the Combustion Institute* 29:2023–2029(2002).

[7] D. Thevenin, O. Gicquel, J. de Charentenay, R. Hilbert, D. Veynante, "Two versus three dimensional direct simulations of turbulent methane flame kernels using realistic chemistry," *Proceedings of the Combustion Institute* 29:2031–2039 (2003).

[8] N. Chakraborty, M. Klein, R.S. Cant, "Stretch effects on displacement speed in turbulent premixed flame kernels in the thin reaction zones regime," *Proceedings of the Combustion Institute* 31: 1385–1392(2007).

[9] K.W. Jenkins, M. Klein, N. Chakraborty, R.S. Cant, "Effects of strain rate and curvature on the propagation of a spherical flame kernel in the thin reaction zones regime," *Combustion and Flame* 145:415–434 (2006).

[10] V.R. Katta, K.Y. Iisu, and W.M. Roquemore, "Local Extinction in an unsteady methane-air jet diffusion flame," *Proceedings of the Combustion Institute* 27:1121-1129 (1998).

[11] P.H. Renard, J.C. Rolon, D. Thevenin, , and S. Candel, "Investigations of heat release, extinction, and time evolution of the flame surface, for a non-premixed flame interacting with a vortex," *Combustion and Flame* 117:189–205 (1999).

A. M. Elbaz, Mohy Mansour & Diaaeldin Mohamed

[12] S.K. Marley, S.J. Danby, W.L. Roberts, M.C. Drake, T.D. Fansler, "Quantification of transient stretch effects on kernel–vortex interactions in premixed methane–air flames," *Combustion and Flame* 154 (2008) 296–309.

[13] C. Arcoumanis, D.R. Hall, and J. H. Whitelaw, "An approach to charge stratification in lean-burn spark-ignition engines," *SAE technical paper* 941878 (1994).

[14] C. Arcoumanis, D.R. Hall, and J.H. Whitelaw, "Optimizing local charge stratification in a lean-burn spark ignition engine," *Proc. Instn. Mech. Engrs, Part D: J. Auto. Eng*. 211:145–154(1997).

[15] C. Arcoumanis, M.R. Gold, J.H. Whitelaw, and H.M. Xu, "Local mixture injection to extend the lean limit of spark-ignition engines," *Exper. Fluids* 26:126–135 (1999).

[16] D.A. Eichenberger, W.L. Roberts, "Effect of unsteady stretch on spark-ignited flame kernel survival," *Combustion and Flame* 118:469–478(1999).

[17] Y. Xiong, W.L. Roberts, M.C. Drake, T.D. Fansler, "Investigation of pre-mixed flame-kernel/vortex interactions via high-speed imaging," *Combustion and Flame* 126:1827–1844 (2001).

[18] Y. Xiong, W.L. Roberts, "Observations on the interaction between a premixed flame kernel and a vortex of different equivalence ratio," *Proceedings of the Combustion Institute*. 29:1687–1693(2002).

[19] D. Thevenin, P.H. Renard, J.C. Rolon, and S. Candel, "Extinction processes during a non-premixed flame / vortex interaction," *Proceedings of the Combustion Institute*. 27:719–726 (1998).

[20] P.H. Renard, J.C. Rolon, D. Thevenin, and S. Candel, "Wrinkling, pocket formation and double premixed flame interaction processes," *Proceedings of the Combustion Institute*. 27:659–666 (1998).

[21] G. Patnaik, and K. Kailasanath, "A computational study of local quenching in flame-vortex interactions with radiative losses," *Proceedings of the Combustion Institute.* 27:711–717 (1998).

[22] H. Reddy and J. Abraham, "A Numerical Study of Vortex Interactions with Flames Developing from Ignition Kernels in Lean Methane/Air Mixtures," *Combustion and Flame* 158 (2011) 401–415.

[23] M.S. Mansour, , N. Peters, L.U. Schrader, "Experimental study of turbulent flame kernel propagation," *Experimental Thermal and Fluid Science*. 32:1396–1404(2008).

[24] B.D. Videto, D.A. Santavicca, "A turbulent flow system for studying turbulent combustion processes," *Combustion Science and Technology* 76 (1991) 159–164.